 DOI: 10.1111/j.1472-4669.2006.00086.x

Alteration of iron-rich lacustrine sediments by dissimilatory iron-reducing bacteria

S. A. CROWE,[1,3] J. A. ROBERTS,[3] C. G. WEISENER[1,2] AND D. A. FOWLE[1,3]

[1]*Great Lakes Institute for Environmental Research, University of Windsor, Windsor, Ontario, Canada N9B 3P4*
[2]*Department of Earth Sciences, University of Windsor, Windsor, Ontario, Canada N9B 3P4*
[3]*Department of Geology, University of Kansas, Lawrence, Kansas 66045, USA*

ABSTRACT

The reduction of Fe during bacterial anaerobic respiration in sediments and soils not only causes the degradation of organic matter but also results in changes in mineralogy and the redistribution of many nutrients and trace metals. Understanding trace metal patterns in sedimentary rocks and predicting the fate of contaminants in the environment requires a detailed understanding of the mechanisms through which they are redistributed during Fe reduction. In this work, lacustrine sediments from Lake Matano in Indonesia were incubated in a minimal media with the dissimilatory iron reducing (DIR) bacterium *Shewanella putrefaciens* 200R. These sediments were reductively dissolved at rates slower than pure synthetic goethite despite the presence of an 'easily reducible' component, as defined by selective extractions. DIR of the lacustrine sediments resulted in the substrate-dependent production of abundant quantities of extracellular polymeric substances. Trace elements, including Ni, Co, P, Si, and As, were released from the sediments with progressive Fe reduction while Cr was sequestered. Much of the initial trace metal mobility can be attributed to the rapid reduction of a Mn-rich oxyhydroxide phase. The production of organo-Fe(III) reveals that DIR bacteria can generate significant metal complexation capacity. This work demonstrates that DIR induces the release of many elements associated with Fe-Mn oxyhydroxides, despite secondary mineralization.

Received 25 May 2006; accepted 25 August 2006

Corresponding author: D. A. Fowle. Tel.: +1 785 864 1955; fax: +1 785 964 5276; e-mail: fowle@ku.edu.

INTRODUCTION

Iron oxyhydroxides are ubiquitous components of surficial materials and are often the dominant redox buffering solid phases in soils and sediments (Heron & Christensen, 1995; Cornell & Schwertmann, 1996). The geochemical behaviour of Fe oxyhydroxides has a profound influence on the global biogeochemical cycling of elements, including carbon, sulfur, nitrogen, and phosphorus in addition to heavy metals and arsenic (Perret *et al.*, 2000; Benner *et al.*, 2002; Stipp *et al.*, 2002). Understanding the behaviour of nutrients and trace metals during biological and abiotic processes that effect iron mineral phase transformations is paramount for predicting their distribution, mobility, and bioavailability in the environment.

In the absence of oxygen, Fe(III) can be used as a terminal electron acceptor (TEA) during microbial respiration (Lovley *et al.*, 2004). In this process, termed enzymatic Dissimilatory Iron Reduction (DIR) (Lovley, 1991), bacteria couple hydrogen and organic carbon oxidation to the reduction of Fe(III). Dissimilatory Fe-reducing bacteria (DIRB) utilize Fe(III) from a wide variety of oxyhydroxide and clay minerals (Lovley *et al.*, 2004). The ensuing reduction of structurally bound Fe(III) to Fe(II) causes the reductive dissolution of these minerals (Lovley *et al.*, 1987; Hering & Stumm, 1990; Grantham *et al.*, 1997; Zachara *et al.*, 2002).

Based on the association between many trace elements and Fe(III) oxyhydroxides, and the tendency for these minerals to be dissolved under suboxic conditions, DIR has often been linked to trace element mobility in the environment. The resultant mobility, however, is controlled by several factors including the nature of the association between the element and the Fe mineral (e.g. isomorphically substituted, adsorbed, included as a discrete mineral phase), a plethora of sorption reactions between the element and the existing sediment and secondary mineralization products (Zachara *et al.*, 2001), by solution chemistry, notably the presence of complexing species such as humic acids (Tessier *et al.*, 1996) and the existence of solution concentration gradients (Hamilton-Taylor & Davison, 1995). Elements commonly

Table 1 Elements associated with Fe oxyhydroxides

Type of association	Elements and valence	References
Substitution for Fe(III)	Ni^{II}, Zn^{II}, Cd^{II}, Al^{III}, Cr^{III}, Ga^{III}, V^{III}, Mn^{III}, Co^{III}, Sc^{III}, Pb^{IV}, Ge^{IV}, Cu^{II}, Si^{IV}, Mg^{II}, Ca^{II}	1
Cation sorption	Pb^{2+}, Zn^{2+}, Cd^{2+}, Hg^{2+}, Cu^{2+}, Ag^{+}, Ni^{2+}, Co^{2+}, Cr^{3+}, Ca^{2+}, Sr^{2+}, Ba^{2+}, Ra^{2+}	2, 3
Anion sorption	PO_4^{3-}, AsO_4^{3-}, VO_4^{3-}, $H_2AsO_3^-$, $H_2BO_3^-$, SeO_3^{2-}, CrO_4^{2-}	2
Present in natural Fe oxides	Al, Cr, Mn, Tl, Cu, Ni	4

associated with Fe oxyhydroxides and, therefore expected to be strongly influenced by DIR, are given in Table 1.

It has been demonstrated that enhanced P mobility in submerged soils was due to ferrihydrite dissolution and the concomitant release of sorbed P (Bostrom *et al.*, 1988). A causal relationship between enhanced mobility and DIR was established for radium (^{226}Ra) in mine tailings (Landa *et al.*, 1991) and As in contaminated lake sediments (Cummings *et al.*, 1999). Detailed experimental work has shown that the biologically induced reductive dissolution of Fe minerals causes the release of strongly bound, isomorphously substituted trace elements such as Ni and Co, from synthetic ferrihydrite (Fredrickson *et al.*, 2001) and goethite (Zachara *et al.*, 2001).

While experiments using monomineralic, synthetic Fe oxyhydroxides can provide fundamental information regarding the rates and mechanisms of DIR, these experimental systems do not adequately replicate the complexity of natural sediments and soils. Accordingly, experiments addressing trace element and nutrient mobility need to be conducted on heterogeneous natural samples, such as lake sediments, in which Fe-bearing minerals are characterized by extensive cation substitution and contain a variety of sorbed trace elements. In this study, trace metal and nutrient release from tropical lake sediments were investigated as a function of DIR.

EXPERIMENTAL

Preparation of sediments and synthetic goethite

Iron-rich sediments (Lake Matano sediment; LMS), produced by the weathering of peridotite bedrock (Golightly, 1981; Crowe *et al.*, 2004) were collected from Lake Matano (Sulawesi Island, Indonesia; 121°20′E, 2°28′S) using a gravity-coring device. LMS from the top 10 cm of the core was freeze-dried and homogenized by mixing, without grinding so as to preserve natural textures, in a 95% ethanol slurry under oxic conditions then evaporated to dryness in a sterile bio-hood. This procedure should render most native consortia nonviable without effecting any mineralogical change.

The mineralogy and texture of LMS were determined using both X-ray diffraction [XRD; Rigaku MiniFlex (Rigaku, The Woodlands, TX, USA) with Cu Kα radiation] and scanning electron microscopy [SEM; Leo 1550 (Carl Zeiss SMT Inc., Thornwood, NY, USA) operated at an accelerating voltage of 20 kV with an energy dispersive spectrometer (EDS)]. Samples for SEM were stub-mounted and gold-sputter-coated for 1.5 min. The major element composition of the sample was determined by X-ray fluorescence (XRF) on a lithium tetraborate fused bead using a Philips PW2440 4 kW instrument (Panalytical Inc., Natick, MA, USA). Accuracy for major and trace elements was within 1 and 5%, respectively, based on the analyses of standard reference materials, and relative precision was within 0.5% determined by repeated analyses of the same fused bead. The surface area of LMS was characterized with a Quantachrome Autosorb1 (Quantachrome Instruments, Boynton Beach, FL, USA) using a five-point BET with nitrogen as the adsorbate gas.

For an experimental reference, a synthetic goethite sample (Gt) was prepared from $FeNO_3{\cdot}9H_2O$ as described in Cornell & Schwertmann (1996). The sample was washed five times in a hydroxylamine hydrochloride solution (0.25 mol L^{-1} $NH_2OH{\cdot}HCl$ in 0.25 mol L^{-1} HCl) and five times in $NaC1O_4$ to remove any residual ferrihydrite (Zachara *et al.*, 2001). Following this treatment the sample was rinsed 5 times in 18 mΩ RO H_2O (Milli-Q, Millipore, Billerica, MA, USA). The washed goethite was then freeze-dried at –50 °C and 100 mbars. Mineralogy was confirmed using XRD and the surface area characterized as described above.

Selective extractions

A suite of selective extractions was used to characterize the nature of Fe oxyhydroxides and potential Mn oxyhydroxides in LMS. Two protocols described by Neaman *et al.* (2004) were used to identify Mn phases. In brief, the first protocol involved mixing 5 mg of LMS with 10 mL of 0.1 M hydroxylamine hydrochloride (pH 3.6) for 2 h. The second protocol involved mixing 10 mg of LMS with 10 mL of 30% H_2O_2 and 0.5 M HNO_3 for 0.5 h. More aggressive extractions including 1.0 M hydroxylamine hydrochloride and citrate dithionite were used to characterize the LMS Fe pool (Poulton & Canfield, 2005). All extractions were conducted in duplicate.

Bacterial culture and growth medium

Cultures of *Shewanella putrefaciens* strain 200R (obtained from J. Haas, Department of Earth Sciences, Western Michigan University) were grown aerobically to the late log phase (18 h) at 32 °C in tryptic soy broth (TSB) (Difco Laboratories, Detroit, MI, USA) with 0.5% yeast extract (Difco Laboratories). The initial cell density in the batch reaction vessels was 10^8 cells mL^{-1} based on visible light adsorption at 600 nm. The bacteria were harvested by centrifugation at 3000 *g* and then

washed three times in an aerobic minimal media and once in anaerobic media of the same composition that had been deoxygenated. The minimal media was comprised of (in mM): KCl, 1.34; NH_4Cl, 28; $CaCl_2$, 0.68; $NaClO_4$, 50; lactate, 24; and PIPES ($C_{16}H_{33}N_4Na_3O_{12}S_4$), 30.

Batch incubations

Thirty-six subsamples with nominal masses of 45 mg (~25 mmol Fe) were allocated to 15 mL polycarbonate test tubes. These batch reaction vessels were inoculated with 10 mL of anaerobic microbial media suspension in an anaerobic chamber (Coy Laboratories Inc., Grass Lake, MI, USA) containing a N_2:CO_2:H_2 (85 : 5 : 10) atmosphere. The reaction vessels were rotated end-over-end at 3.5×10^{-2} and incubated at 30 °C in the absence of sunlight. Batch sampling was conducted by sacrificing selected vessels, in duplicate, periodically over a period of 16 days. Solutions were filtered through a 0.2-μm filter and Fe(II)/Fe(III) (Viollier *et al.*, 2000), alkalinity (Sarazin *et al.*, 1999), and pH were determined within the chamber immediately after filtration. Spectrophotometric measurements were conducted using a HACH DR2010 spectrophotometer (1 cm path length) (USA HACH Company, Loveland, CO, USA) situated within the anaerobic chamber. The Fe(II)/Fe(III) measurements were conducted within the chamber to minimize the potential oxidation of Fe(II) by O_2 from the atmosphere. The ferrozine reagent was added to filtered samples immediately (< 1 min) after filtration. Following the addition of the ferrozine reagent the sample was mixed and allowed to equilibrate for 5 min before the absorbance was measured. The hydroxylamine reductant was allowed to react with the sample for 30 min before addition of the pH buffer to allow sufficient time for the reduction of soluble reactive Fe(III) species. The absorbance for Fe(III) measurements was measured immediately after the addition of the pH buffer. Samples for trace element determination were acidified to 1% HNO_3 (using 50% subboiling distilled HNO_3) and stored at 4 °C until ICP-MS analysis. Trace element concentrations, including P, in solution were determined by ICP-MS using a Thermo-Elemental X7 (Thermoelectron Corp., Walthorn, MA, USA) with a collision cell. Accuracy and precision of ICP-MS determinations are better than 2% determined by replicate analyses of standard reference water SLRS-4. Aliquots of incubated solids were preserved for SEM using a chemical critical point drying method (Bennett *et al.*, in press) to fix biological tissues and preserve cell morphology. The remaining solid was reserved for XRD analysis (as described above) and freeze-dried at −50 °C and 100 mbars. Geochemical modelling was conducted using JChess with the Chess thermodynamic database (van der Lee, 1993).

Voltammetry

Voltammetric measurements [AIS Instruments (Flemington, NJ, USA) DLK potentiostat] were conducted with a 50 μm radius Au/Hg amalgam working electrode (Brendel & Luther, 1995), a Ag/AgCl reference and a 1-mm Pt wire counter. Previous workers have shown that organo-Fe(III) complexes generate a characteristic current vs. time peak in voltammograms (Brendel & Luther, 1995; Taillefert *et al.*, 2000; Carey & Taillefert, 2005). These organo-Fe(III) complexes were detected using cathodic stripping voltammetry (CSV) (Taillefert *et al.*, 2000). In this technique the organo-Fe(III) complex is deposited on the Hg surface at a potential of −0.05 V (vs. saturated Ag/AgCl). The complex is then reduced at the Hg surface by applying a cathodic scan. The current that results from this reaction is monitored and plotted vs. applied potential (Fig. 3A inset). The two scans (Fig. 3A inset) were conducted after 7 days of incubation with (blue) and without (red) deposition of the organo-Fe(III) complex at a potential of −0.05 V vs. Ag/AgCl. The difference in the peak current at −1.43 V vs. Ag/AgCl [which results from the reduction of Fe(II) to Fe(0)], with and without deposition, confirms that the broad peak at ~−0.40 V vs. Ag/Cl is due to the electrochemical reduction of Fe(III) to Fe(II).

Synchrotron based micro-XRF

Micro-XRF data (Fig. 2) were acquired on beamline X26-A at the National Synchrotron Light Source (NSLS), Brookhaven National Laboratory (Upton, New York). Beamline X26-A is capable of micron-scale spatial resolution. The detector used at X26-A was a Microspec Wavelength Dispersive Spectrometer (Acton Research Corp., Acton, MA, USA) and a Bruker SMART 1500 CCD array system (Bruker Axs Inc., Madison, WI, USA).

RESULTS AND DISCUSSION

Characterization of LMS

XRD spectra reveal that the mineralogy of LMS is dominated by goethite (Fig. 1A), and contains minor amounts of quartz. Scanning electron microscopy (Fig. 1B) revealed that LMS is comprised largely of acicular fibers of up to 1 μm in length and less than 100 nm in width. This morphology is characteristic of fine-grained goethite (Cornell & Schwertmann, 1996) and is consistent with the XRD analysis. The bulk chemical composition of the sample is presented in Table 2. Specific surface areas of LMS and Gt were similar, with measured values of 49.15 $m^2\ g^{-1}$ and 52.3 $m^2\ g^{-1}$, respectively. The surface area of Gt is similar to the surface area of 55 $m^2\ g^{-1}$ reported for medium surface area goetite (Roden & Zachara, 1996). The value of 49.15 $m^2\ g^{-1}$ obtained for LMS surface area is relatively high for goethite-rich sediments (Roden, 2004). Although the mineralogy of the sediment is dominated by goethite (see below), the surface area measurements for LMS represent the mean contribution from all of the phases present. The surface area of LMS is less than 10% lower than Gt and suggests that Gt and LMS should exhibit broadly comparable sorption capacities. However, as the phase composition of LMS is different than Gt (see below), the specific chemical affinities of surface sites for Fe(II) and other divalent cations may be different.

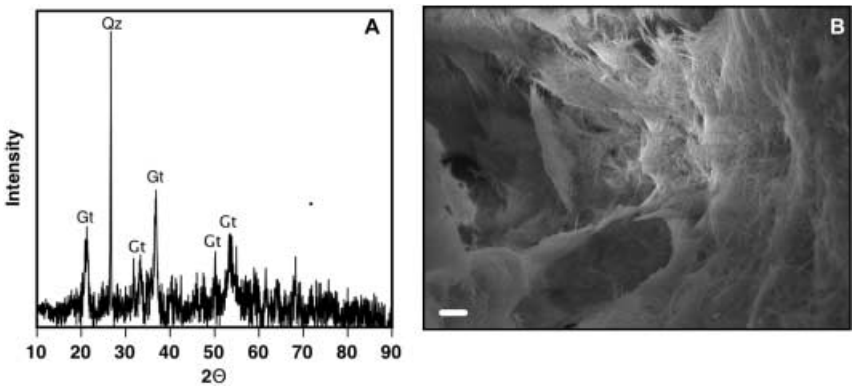

Fig. 1 (A) X-ray diffraction patterns of Lake Matano sediment (LMS) (Gt = goethite; Qz = quartz). (B) SEM photomicrograph of LMS before incubation with bacteria (scale bar is 2 μM).

Table 2 Lake Matano sediment composition determined by XRF after lithium tetraborate fusion (accuracy < 5%, precision < 0.5%)

Element	Concentration (wt %)	Element	Concentration (p.p.m.)
SiO_2	26.60	Co	541
TiO_2	0.400	Ni	9800
Al_2O_3	8.00	V	165
Fe_2O_3	43.40		
MnO	0.200		
MgO	4.00		
CaO	0.70		
Na_2O	0.20		
K_2O	0.50		
P_2O_5	0.400		
Cr_2O_3	0.940		

Extractions that have been previously optimized to operationally select for Mn oxyhydroxides demonstrate a Mn-rich phase present in LMS (Table 3). Of the total Mn pool 15 and 36% were dissolved by the 0.1 M hydroxylamine HCl and H_2O_2 extractions, respectively. The 0.1 M hydroxylamine HCl and H_2O_2 extractions also dissolved Fe, however, the ratios of Mn:Mn+Fe (Table 3) are high and consistent with the existence of discrete Mn-rich phases in LMS. The larger fraction of Mn dissolved by the H_2O_2 compared with the 0.1 M hydroxylamine HCl extraction is consistent with the presence of a refractory phase such as lithiophorite in LMS (Neaman *et al*., 2004). Maps of Kα florescence intensity (Fig. 2) demonstrate that Mn in LMS exists both as discrete phases (red regions) and incorporated into Fe minerals (pink regions). The extractions optimized to functionally characterize the LMS Fe pool suggest that 16.2% of the Fe in LMS is 'easily reducible' Fe oxyhydroxides such as ferrihydrite or lepidocrocite (Poulton & Canfield, 2005) and 39.2% of the LMS Fe pool consists of 'reducible' minerals including goethite, haematite and akaganeite (Poulton & Canfield, 2005).

Reductive dissolution and organo-Fe(III) production

In both Gt and LMS incubations, the initial pH was 6.56 with an increase of < 0.1 units over the duration of the experiment. Alkalinity in the LMS and Gt incubations increased systematically from 4.5 mM at 44 h to a maximum of ~8 mM at day 10 and dropped sharply to 5.5 mM at 13 days. Aqueous Fe(II) and Fe(III) concentrations increased during incubation (Fig. 3). Surface area normalized rates of reductive dissolution were obtained by calculating linear regressions using the aqueous Fe(II) concentrations in the first 6 days of incubation (Roden, 2003). With a surface area normalized first order rate constant of $1.4 \times 10^{-3} \pm 0.4 \times 10^{-3}$ μmol m^{-2} s^{-1}, LMS was dissolved at a rate slower than Gt ($2.6 \times 10^{-3} \pm 1.1 \times 10^{-3}$ μmol m^{-2} s^{-1}), at the 95% confidence level, despite the existence of an 'easily reduced' component defined by the selective extractions.

These rates of dissolution may be used to approximate rates of reduction. However, these rates are based strictly on aqueous Fe(II) and therefore underestimate rates of reduction as some Fe(II) would have been sequestered by the solid phase and is not accounted for. The rates of dissolution observed here for LMS and Gt are broadly comparable to the rates of reduction observed for minerals of similar specific surface areas (Roden, 2003).

It is well established that the substitution of trace divalent and trivalent cations for Fe(III) in iron oxyhydroxides influences

Table 3 Selective extractions [extractions are expected to have a precision of < 5% (Poulton & Canfield, 2005)]

Extraction	Extractable metal (mmol g^{-1})		Fraction of total (%)		Mn/(Mn+Fe)
	Fe	Mn	Fe	Mn	
0.1 M hydroxylamine HCl	0.003	0.004	0.06	15	0.57
H_2O_2	0.021	0.01	0.39	36	0.32
1 M hydroxylamine HCl	0.88	0.015	16.2	52	0.017
Citrate dithionite	3.01	0.016	55.4	57	0.005

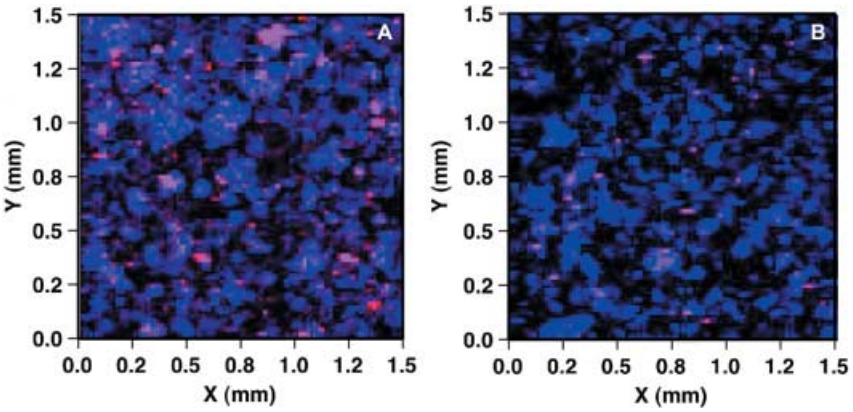

Fig. 2 X-ray fluorescence maps. (A) Lake Matano sediment (LMS) before incubation. (B) LMS after 16 days incubation. Increases in the intensity of the colours blue and red represent an increase in the relative abundance of Fe and Mn, respectively (i.e. pink zones represent Mn associated with Fe, whereas red areas are discrete Mn phases).

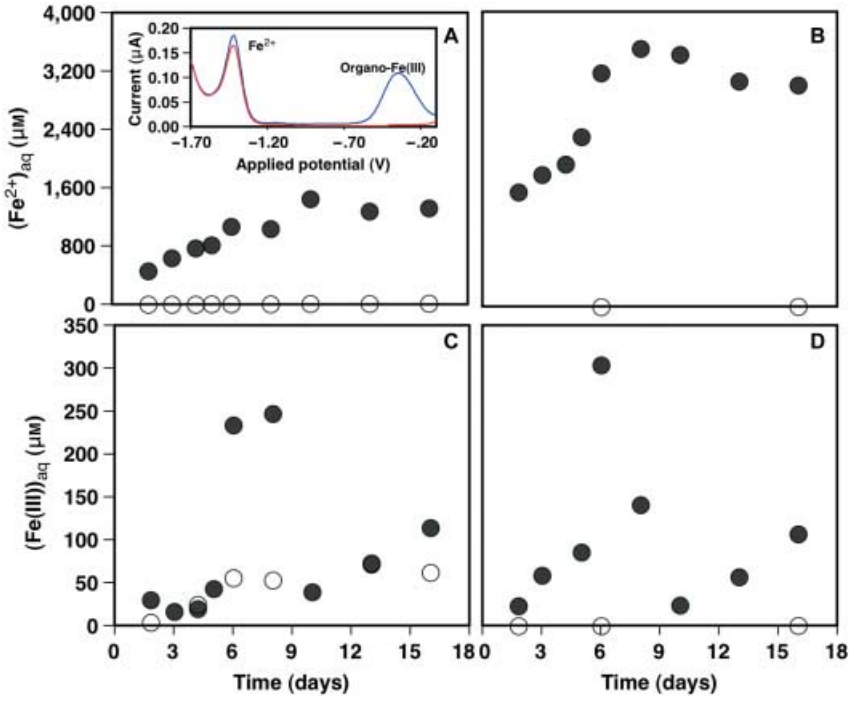

Fig. 3 Fe speciation vs. time. (A) concentration of aqueous Fe^{2+} (μM) in Lake Matano sediment (LMS) incubations (inset) average of 3 square wave voltammetric scans demonstrating the coexistence of aqueous Fe^{2+} and organo-Fe(III) complexes, blue = with deposition at –0.1 V, red = no deposition at –0.1 V (B) concentration of aqueous Fe^{2+} (μM) in Gt incubations (C) concentration of aqueous Fe^{3+} (μM) in LMS incubations (D) concentration of aqueous Fe^{3+} (μM) in Gt incubations. Closed circles are inoculated LMS and Gt and open circles are 'uninoculated' controls.

the reactivity of these minerals by altering the bulk crystal chemistry (Trolard & Tardy, 1987; Gerth, 1990), surface chemistry (Ainsworth *et al.*, 1989), solubility (Trolard & Tardy, 1987), and dissolution kinetics (Torrent *et al.*, 1987; Schwertmann, 1991). It has been shown that the substitution of specific cations influences the rate and extent of microbially induced reductive dissolution of Fe(III) oxyhydroxide minerals (Zachara *et al.*, 1998, 2001; Bousserrhine *et al.*, 1999; Fredrickson *et al.*, 2001; Kukkadapu *et al.*, 2001). It is possible that the precipitation of Cr and Al species on Fe oxyhydroxide surfaces may slow the rate of reduction in LMS compared to Gt (Bousserrhine *et al.*, 1999). In other studies (Kukkadapu *et al.*, 2001), it was found that natural Al substituted (15%) goethite from Atlantic coastal plain sediments was reduced at twice the rate of pure synthetic goethite by DIRB (*Shewanella putrefaciens* CN32). It was postulated that the surface passivation effect of Al was counterbalanced by other factors such as increased structural disorder or Al adsorption to other trace mineral constituents. The slower rate of reduction for LMS compared to Gt suggests that the presence of trace constituents impedes Fe reduction despite increasing structural disorder.

The high aqueous Fe (III) (~300 μM) concentrations (Fig. 3C,D) provide evidence for Fe(III) complexation. These concentrations are well above those expected based on the solubility of the aqueous free ion Fe^{3+} (9.6×10^{-20} M) or those for the aqueous ferric hydroxide species $Fe(OH)_3$ 1.1×10^{-12} M. Voltammetric scans (Fig. 3A inset) conducted in parallel reaction vessels reveal peaks consistent with the production of Fe(III) binding ligands during DIR of LMS by *S. putrefaciens* 200R. Organic-Fe(III) peaks could not be detected in control vessels that were not inoculated with *S. putrefaciens*. Current

conceptual models for the mechanisms through which DIRB gain access to insoluble Fe oxides include direct transfer of electrons from outer membrane cytochromes to mineral surfaces, the use of chelating agents to dissolve Fe(III), and electron shuttling via natural organic matter or bacterial exudates (Nevin & Lovley, 2002). Recently, it has been demonstrated that electron transfer to extracellular substances can be facilitated through electrically conductive pilli or 'nanowires' (Reguera *et al.*, 2005; Gorby *et al.*, 2006). Consistent with the hypothesis of Carey and Taillefert (Carey & Taillefert, 2005) we suggest that the production of an organo-Fe(III) species during the respiration of LMS is the result of a strategy by some DIR bacteria to access Fe(III) from minerals. We propose that the production of ligands, perhaps a soluble component of EPS, during DIR would stabilize aqueous species and enhance trace metal mobility in aquatic sediments. At this point it is not feasible to completely rule out the possibility that these ligands may be generated due to cell lysis after death. However, the fact that most of the trace metal release occurred during or before the accumulation of significant aqueous Fe(II) suggests that metal release was largely the result of microbial activity and not a passive response to an increase in cellular debris.

Secondary mineralization and EPS production

Characterization of incubated LMS and Gt samples using SEM showed evidence of secondary mineral precipitation (Fig. 4A). These precipitates are small euhedral crystallites (~0.2 um), which occur clustered near cells but were too small to compositionally characterize using EDS. Thermodynamic equilibrium calculations have been used to predict potential secondary minerals. The results of these calculations are reported as saturation indices (SI) (Table 4). In this work SI is defined as:

$$\mathrm{SI} = \log\frac{[IAP]}{[K_{\mathrm{SP}}]}$$

where IAP is the ion activity product and K_{SP} is the solubility product for a given ion pair. Based on these calculations it appears that siderite ($FeCO_3$) may have precipitated throughout the duration of the experiment and therefore likely constitutes the major solid-phase sink for reduced Fe.

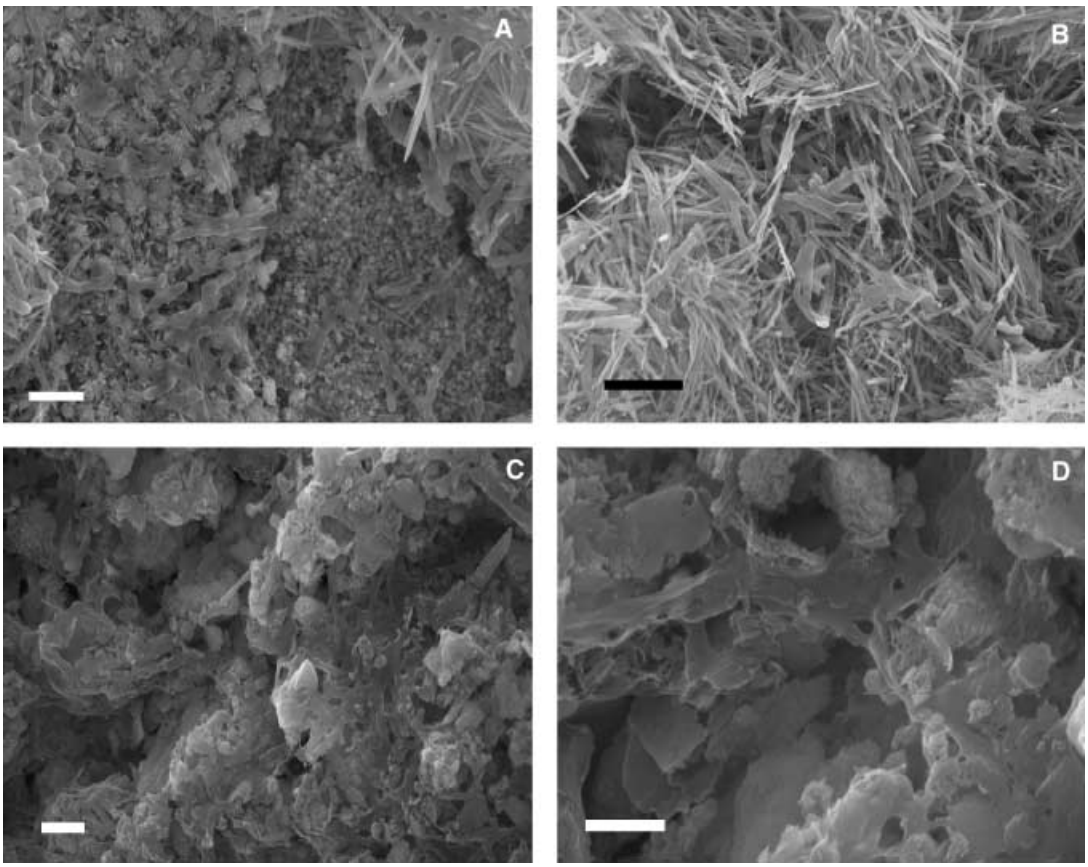

Fig. 4 (A) Secondary mineralization in Gt after 10 days, note the fine-grained equi-dimensional mineral precipitate that occupies most of the field of view and the larger acicular goethite crystals (scale bar = 2 μM). (B) Gt after 16 days, note the absence of polymeric substances and the occurrence of grouped cells (scale bar = 3 μM). (C) Lake Matano sediment (LMS) incubations after 10 days, note the abundance of extracellular polymeric substances (EPS) that connect groups of cells (scale bar = 2 μM). (D) A higher magnification of LMS after 10 days incubation (scale bar = 1 μM).

Table 4 Saturation indices calculated for various solid species of interest at three times over the course of incubations

Mineral name	Chemical formula	Day 2	Day 10	Day 16
	Co_2SiO_4	3.23	3.86	3.71
	$MnHPO_4$	2.31	3.02	3.01
Siderite	$FeCO_3$	0.23	0.93	0.77
Minnesotaite	$(Fe,Mg)_3Si_4O_{10}(OH)_2$	–0.59	1.26	1.34
Rhodochrosite	$MnCO_3$	–0.76	–0.30	–0.58
	SiO_2(am)	–0.88	–0.82	–0.79
Calcite	$CaCO_3$	–1.29	–0.99	–1.19
	Ni_2SiO_4	–1.37	–0.81	–0.82
Magnetite	Fe_3O_4	< –3	< –3	0.370
Vivianite	$Fe_3(PO4)_2(H_2O)_8$	< –3	< –3	– 2.68

Magnetite (Fe_3O_4) became saturated towards the end of the experiment and may become a more important sink for Fe over long periods of time. Vivianite ($Fe_3(PO4)_2{\cdot}(H_2O)_8$) remained undersaturated throughout the period of incubation, suggesting it is neither an important sink for reduced Fe or P under our experimental conditions. Instead, $MnHPO_4$ was supersaturated throughout the experiment, although it should be noted that shifting the pH of the system above pH 7 would provide thermodynamically favourable conditions for the formation of vivianite. This suggests that $MnHPO_4$ may be an important sink for P and Mn in reducing environments like lacustrine sediments, where the pH can be below 7, despite the much greater abundance of Fe. Amorphous Si remained undersaturated throughout the incubations, suggesting that diatoms present in the sediment could dissolve during Fe reduction. This may be the origin of some of the Si that accumulated in the aqueous phase over the course of the incubations. Recently, a link has been drawn between rapid clay mineral formation and Fe, Al oxide-rich sediments (Michalopoulos & Aller, 2004). Presumably, the enhanced clay-mineral formation rates in metal oxide-rich sediments result from the ample flux of cations induced by the reductive dissolution of Fe oxides. In our experiments the clay mineral minnesotaite was supersaturated throughout the experiment, suggesting that the simultaneous dissolution of amorphous Si and dissimilatory Fe reduction in Fe-rich sediments could lead to rapid, low-temperature, clay mineral formation. Considering that minnesotaite is a principal component in unaltered banded iron formations (Walker *et al.*, 1983), and the potential importance of DIR in the formation of the reduced constituents in BIFs, the possible relationship between DIR and minnesotaite formation should be further investigated. For example, if minnesotaite were to precipitate during the early stages of diagenesis, it could form an important nonreactive sink for Fe^{2+}, enhancing the potential release of P from sediments and/or decoupling reduced Fe from C. The silicon released during DIR could also play an important role in regulating trace element release via sorption and interlayer capture in secondary clay minerals formed as iron reduction progresses.

Micro-organisms attach to both the original Fe oxyhydroxides and the secondary precipitates in small groups as well as in multicellular assemblages associated with extracellular polymeric substances (EPS). Micro-organisms on LMS, particularly at the end of the incubation, occur as large surface-adherent groups of cells coated in EPS (Fig. 4C). These putative biofilms can cover extensive areas of the LMS surface. Cells on the Gt surface also occur in groups but EPS is scarce (Fig. 4B). Cell assemblages are smaller and are more discretely distributed on the Gt surface. The production of EPS in the presence of LMS but not Gt is consistent with previous observations that the production of EPS by *S. putrefaciens* depends on the composition of the electron acceptor substrate (Little *et al.*, 1997; Larsen *et al.*, 1998) and may be related to the presence of Mn oxyhydroxides. The extensive EPS-cell assemblages observed on LMS may impede Fe reduction by forming a barrier between the mineral/bacterial surfaces and the bulk solution. Thus, mass transfer of reduction products out of these microenvironments may impose both kinetic and thermodynamic barriers to Fe reduction (Roden & Zachara, 1996; Urrutia *et al.*, 1999; Welch *et al.*, 1999).

Trace element liberation

The aqueous concentrations of several trace elements of interest, Mn, Ni, Co, As, P, and Si, were found to increase with progressive Fe reduction. In contrast Cr and Ca decreased with progressive Fe reduction (Table 5, Fig. 5).

To a first approximation the release of Mn, Co and Ni can be attributed to the reductive dissolution of Fe oxyhydroxides. However, the release of these elements in advance of significant DIR (< 44 h) is likely due to the reductive dissolution of a phase more readily reduced than the Fe oxyhydroxide (e.g. MnO_2). This is consistent with the 0.1 M hydroxylamine HCl and H_2O_2 extractions which identified a Mn-rich phase in LMS (Table 3) and with previous work (Quantin *et al.*, 2001, 2002) that documented a Co- and Ni-bearing MnO_2 phase in lateritic soils. Quantin *et al.* (2001, 2002) found that this MnO_2 phase was reduced prior to Fe during fermentation-induced weathering. Comparison of Kα XRF maps of the LMS starting material with that of material after 16 days of incubation shows a decrease in the abundance of discrete Mn phases (Fig. 3). The approximately equivalent dissolution of Mn

Table 5 Mass balance for trace element release (at maximum aqueous concentrations)

Element	Aqueous total (%)
Fe	5.86
Mn	33
Ni	5.4
Co	3.0
P	44
As	NA*
Cr	0.1

*Arsenic was not determined in LMS.

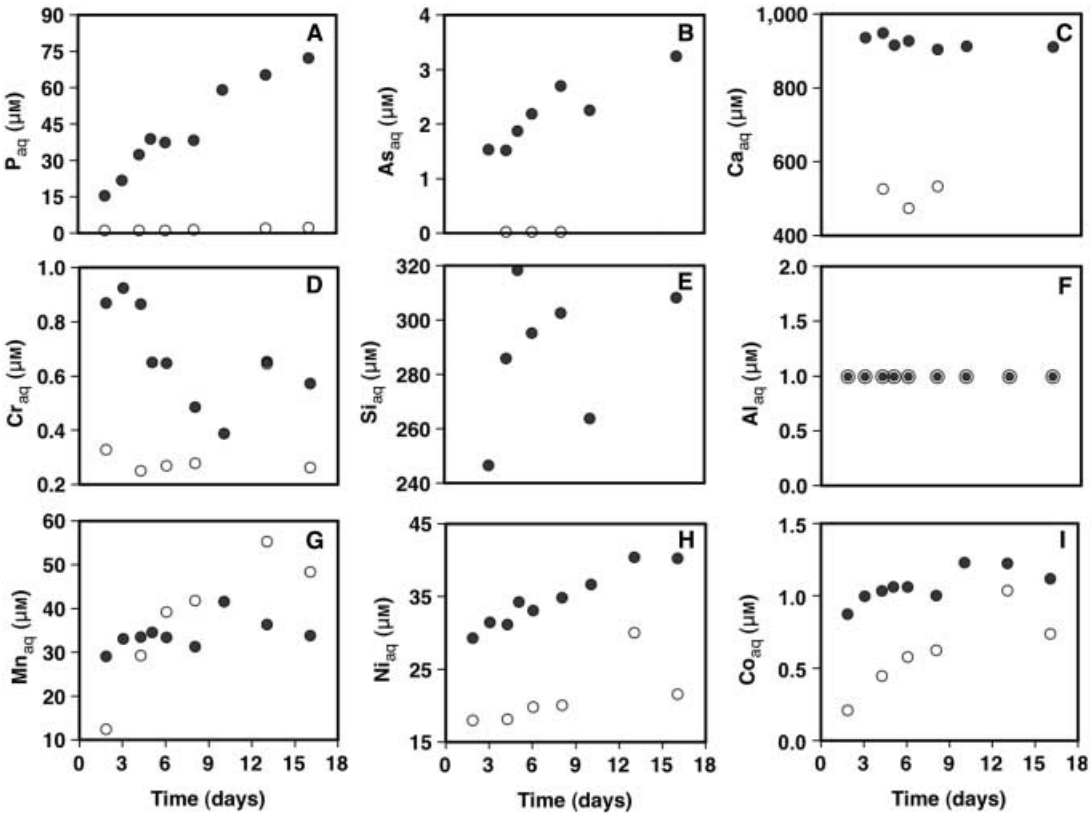

Fig. 5 Aqueous concentrations of trace elements (μM) in Lake Matano sediment (LMS) incubations vs. time. Closed circles are inoculated LMS and open circles are uninoculated controls.

in uninoculated LMS (Fig. 5G) can be attributed to either abiotic reduction by organic matter or reduction by persistent indigenous cultures not rendered sterile by evaporation under ethanol.

Over the duration of the 16-day experiment, nearly 50% of the total P was liberated from LMS. Arsenic followed a similar release trend. Equilibrium speciation calculations predict that the dominant aqueous As species were $H_2AsO_4^-$ and $HAsO_4^{2-}$, suggesting that As released from LMS would not have been reduced. Incubations with Gt showed a rapid decrease (1 day; data not shown) of aqueous P concentrations to below our detection limit (~2 μM). As P was not added to the minimal media, the aqueous P observed in Gt samples must have originated from the bacterial inoculums.

Silicon was released up to 1.5% of its total abundance. Presumably, this represents a reactive fraction of silica, potentially diatoms, and Si incorporated into Fe oxyhydroxides. The concentration of aqueous Cr increased rapidly within the first 44 h, consistent with desorption of soluble, surface-bound chromate or the release of Cr(VI) from dissolution of the Mn-rich phase. Reduction of Cr(VI) to the much less soluble Cr(III) by Fe(II) would explain the decrease in aqueous Cr with DIR (Hansel *et al.*, 2003). Equilibrium speciation calculations predict that the stable Cr species is the mineral eskolaite (Cr_2O_3) (although an amorphous $Cr(OH)_{3(s)}$ would likely be kinetically favoured) and therefore support this hypothesis. Aqueous calcium concentrations also decreased with progressive DIR. This was likely due to the precipitation of carbonate phases as a result of increased alkalinity from lactate oxidation. As the solution is undersaturated with respect to calcite based on equilibrium calculations, it is possible that Ca may be co-precipitated with Fe/Mn carbonates such as siderite. Al substitution in goethite is likely significant, however, aqueous Al concentrations remained below our detection limits (~1 μM) and there appears to be no release of Al during DIR. As a result, Al redistribution must occur largely within the solid phase.

A 1 : 1 relationship between the release of a given trace element and dissolution of Fe is analogous to congruent dissolution in pure mineral systems. When the fraction of a given trace element is plotted as a function of the total Fe dissolved (Fig. 6) it is apparent that the initial release of trace metals is more extensive than Fe as noted above. With the progressive Fe reduction, Mn and Ni release rates approach the rate of Fe dissolution. In contrast, Co release is proportionally lower. The difference in release rates between Co and Ni demonstrates that these metals are fractionated during DIR.

CONCLUSIONS

Lake Matano sediment (LMS) is reductively dissolved at rates slower than synthetic goethite despite the presence

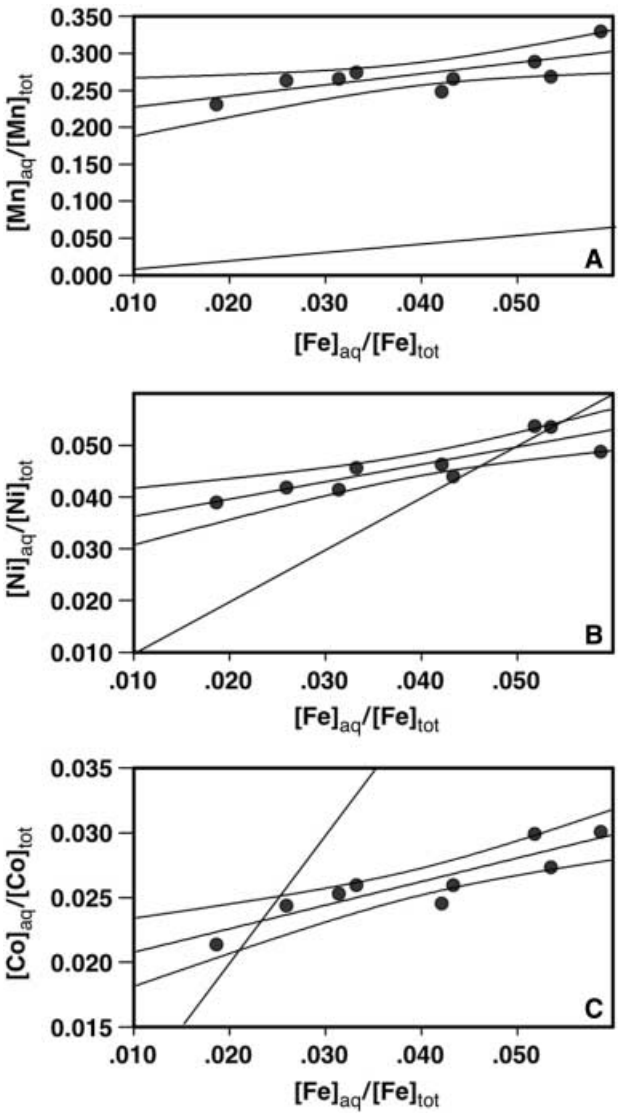

Fig. 6 Trace metal release as a function of Fe dissolution plotted as the concentration of aqueous metal $[Me]_{aq}$ over the total metal concentration $[Me]_{tot}$. Note that $[Fe]_{aq}$ is the sum of aqueous Fe^{2+} and aqueous Fe^{3+}. The single solid line indicates congruent (1:1) release. (A) Mn. (B) Ni. (C) Co. Error margins on the regression represent 95% confidence intervals.

of oxyhydroxide phases that are more readily reduced by chemical reagents. In LMS, mixed Fe/Mn oxyhydroxides provide a reactive reservoir of mobile trace metals. Natural oxyhydroxide minerals elicit different biological responses than pure synthetic counterparts, for example the production of EPS during DIR. This implies that the impact of DIR on sediment and soil geochemistry and mineralogy is highly dependent on the specific composition of the Fe substrate. This complicates both the use of sediment trace element chemistry for interpretation of palaeoenvironmental conditions and the prediction of contaminant mobility in aquatic environments. The ability of DIR bacteria to generate metal complexation capacity during respiration suggests that biogenic ligand production should be considered a potential mechanism to induce trace metal mobility and potentially alter metal bioavailability in sediments and aquifers under suboxic conditions.

ACKNOWLEDGEMENTS

This research was supported by OIT, NSERC, PREA, and CRC grants (Fowle), Petroleum Research Fund Grant No. 38868-G2 (Roberts), and NSF Grant EAR no. 0230204 (Roberts). Use of the beamline X26A at the NSLS was supported by DOE under Contract No. DE-AC02-98CH10886. The manuscript significantly benefited from the contributions of three anonymous reviewers and editorial comments from K. Konhauser. We gratefully acknowledge D. Haffner, R. McKneely, P. Hehanussa and D. Roy for the collection of sediment samples from Indonesia, and J. Gagnon and B. Fryer for help with the ICP-MS analyses. We would also like to thank A. Mucci, B. Sundby, A. O'Neill and C. Magen for informative discussions throughout the course of the manuscript preparation.

REFERENCES

Ainsworth CC, Zachara JM, Smith SC (1989) Carbazole sorption by surface and subsurface materials – influence of sorbent and solvent properties. *Soil Science Society of America Journal* **53**, 1391–1401.

Benner SG, Hansel CM, Wielinga BW, Barber TM, Fendorf S (2002) Reductive dissolution and biomineralization of iron hydroxide under dynamic flow conditions. *Environmental Science and Technology* **36**, 1705–1711.

Bennett PC, Engel AS, Roberts JA (2006) Counting and imaging bacteria on mineral surfaces. In Methods of Investigating Microbial–Mineral Interactions, CMS Workshop Lectures (eds. Maurice JPA, Warren A). The Clay Mineral Society, Chantilly, Vol. **14**, 37–78.

Bostrom B, Andersen JM, Fleischer S, Jansson M (1988) Exchange of phosphorus across the sediment–water interface. *Hydrobiologia* **170**, 229–244.

Bousserrhine N, Gasser UG, Jeanroy E, Berthelin J (1999) Bacterial and chemical reductive dissolution of Mn-, Co-, Cr-, and Al-substituted goethites. *Geomicrobiology Journal* **16**, 245–258.

Brendel PJ, Luther GW (1995) Development of a gold amalgam voltammetric microelectrode for the determination of dissolved Fe, Mn, O_2, and S(-II) in porewaters of marine and fresh-water sediments. *Environmental Science and Technology* **29**, 751–761.

Carey E, Taillefert M (2005) The role of soluble Fe(III) in the cycling of iron and sulfur in coastal marine sediments. *Limnology and Oceanography* **50**, 1129–1141.

Cornell RM, Schwertmann U (1996) *The Iron Oxides: Structure, Properties, Reactions, Occurrences and Uses*. Wiley VCH, Weinheim, Germany.

Crowe SA, Pannalal SJ, Fowle DA, Cioppa MT, Symons DTA, Haffner GD, Fryer BJ, McNeely R, Sundby B, Hehanussa PE (2004) Biogeochemical cycling in Fe-rich sediments from Lake Matano, Indonesia. *13th International Symposium on Water–Rock Interaction*, 1185–1189.

Cummings DE, Caccavo F, Fendorf S, Rosenzweig RF (1999) Arsenic mobilization by the dissimilatory Fe(III)-reducing

bacterium *Shewanella alga* BrY. *Environmental Science and Technology* **33**, 723–729.
Fredrickson JK, Zachara JM, Kukkadapu RK, Gorby YA, Smith SC, Brown CF (2001) Biotransformation of Ni-substituted hydrous ferric oxide by an Fe(III)-reducing bacterium. *Environmental Science and Technology* **35**, 703–712.
Gerth J (1990) Unit-cell dimensions of pure and trace metal-associated goethites. *Geochimica et Cosmochimica Acta* **54**, 363–371.
Golightly JP (1981) Nickeliferous laterite deposits. *Economic Geology* 75th Anniversary Volume, 710–735.
Gorby YA, Yanina S, McLean JS, Rosso KM, Moyles D, Dohnalkova A, Beveridge TJ, Chang IS, Kim BH, Kim KS, Culley DE, Reed SB, Romine MF, Saffarini DA, Hill EA, Shi L, Elias DA, Kennedy DW, Pinchuk G, Watanabe K, Ishii S, Logan B, Nealson KH, Fredrickson JK (2006) Electrically conductive bacterial nanowires produced by *Shewanella oneidensis* strain MR-1 and other microorganisms. *Proceedings of the National Academy of Sciences of the United States of America* **103**, 11358–11363.
Grantham MC, Dove PM, DiChristina TJ (1997) Microbially catalyzed dissolution of iron and aluminium oxyhydroxide mineral surface coatings. *Geochimica et Cosmochimica Acta* **61**, 4467–4477.
Hamilton-Taylor J, Davison W (1995) Redox-driven cycling of trace elements in lakes. In *Physics and Chemistry of Lakes* (eds Lerman A, Imboden D, Gat J). Springer-Verlag, Berlin, Germany, pp. 217–263.
Hansel CM, Wielinga BW, Fendorf SR (2003) Structural and compositional evolution of Cr/Fe solids after indirect chromate reduction by dissimilatory iron-reducing bacteria. *Geochimica et Cosmochimica Acta* **67**, 401–412.
Hering JG, Stumm W (1990) Oxidative and reductive dissolution of minerals. *Reviews in Mineralogy* **23**, 427–465.
Heron G, Christensen TH (1995) Impact of sediment-bound iron on redox buffering in a landfill leachate polluted aquifer (Vejen, Denmark). *Environmental Science and Technology* **29**, 187–192.
Kukkadapu RK, Zachara JM, Smith SC, Fredrickson JK, Liu CX (2001) Dissimilatory bacterial reduction of Al-substituted goethite in subsurface sediments. *Geochimica et Cosmochimica Acta* **65** (17), 2913–2924.
Landa ER, Phillips EJP, Lovley DR (1991) Release of Ra-226 from uranium mill tailings by microbial Fe(iii) reduction. *Applied Geochemistry* **6**, 647–652.
Larsen I, Little B, Nealson KH, Ray R, Stone A, Tian JH (1998) Manganite reduction by *Shewanella putrefaciens* MR-4. *American Mineralogist* **83**, 1564–1572.
van der Lee J (1993) *CHESS, Another Speciation and Surface Complexation Computer Code*. CIG-Ecole des Mines de Paris, Fountainebleau, France.
Little BJ, Wagner PA, Lewandowski Z (1997) Spatial relationships between bacteria and mineral surfaces. *Geomicrobiology: Interactions Between Microbes and Minerals* **35**, 123–159.
Lovley DR (1991) Dissimilatory Fe(III) and Mn(IV) Reduction. *Microbiological Reviews* **55**, 259–287.
Lovley DR, Stolz JF, Nord GL, Phillips EJP (1987) Anaerobic production of magnetite by a dissimilatory iron-reducing microorganism. *Nature* **330**, 252–254.
Lovley DR, Holmes DE, Nevin KP (2004) Dissimilatory Fe(III) and Mn(IV) reduction. *Advances in Microbial Physiology* **49**, 219–286.
Michalopoulos P, Aller RC (2004) Early diagenesis of biogenic silica in the Amazon delta: alteration, authigenic clay formation, and storage. *Geochimica et Cosmochimica Acta* **68**, 1061–1085.
Neaman A, Waller B, Mouele F, Trolard F, Bourrie G (2004) Improved methods for selective dissolution of manganese oxides from soils and rocks. *European Journal of Soil Science* **55**, 47–54.
Nevin KP, Lovley DR (2002) Mechanisms for Fe(III) oxide reduction in sedimentary environments. *Geomicrobiology Journal* **19**, 141–159.
Perret D, Gaillard JF, Dominik J, Atteia O (2000) The diversity of natural hydrous iron oxides. *Environmental Science and Technology* **34**, 3540–3546.
Poulton SW, Canfield DE (2005) Development of a sequential extraction procedure for iron: implications for iron partitioning in continentally derived particulates. *Chemical Geology* **214**, 209–221.
Quantin C, Becquer T, Rouiller JH, Berthelin J (2001) Oxide weathering and trace metal release by bacterial reduction in a New Caledonia Ferralsol. *Biogeochemistry* **53**, 323–340.
Quantin C, Becquer T, Berthelin J (2002) Mn-oxide: a major source of easily mobilisable Co and Ni under reducing conditions in New Caledonia Ferralsols. *Comptes Rendus Geoscience* **334**, 273–278.
Reguera G, McCarthy KD, Mehta T, Nicoll JS, Tuominen MT, Lovley DR (2005) Extracellular electron transfer via microbial nanowires. *Nature* **435**, 1098–1101.
Roden EE (2003) Fe(III) oxide reactivity toward biological versus chemical reduction. *Environmental Science and Technology* **37**, 1319–1324.
Roden EE (2004) Analysis of long-term bacterial vs. chemical Fe(III) oxide reduction kinetics. *Geochimica et Cosmochimica Acta* **68**, 3205–3216.
Roden EE, Zachara JM (1996) Microbial reduction of crystalline iron(III) oxides: Influence of oxide surface area and potential for cell growth. *Environmental Science and Technology* **30**, 1618–1628.
Sarazin G, Michard G, Prevot F (1999) A rapid and accurate spectroscopic method for alkalinity measurements in sea water samples. *Water Research* **33**, 290–294.
Schwertmann U (1991) Solubility and dissolution of iron-oxides. *Plant and Soil* **130**, 1–25.
Stipp SLS, Hansen M, Kristensen R, Hochella MF, Bennedsen L, Dideriksen K, Balic-Zunic T, Leonard D, Mathieu HJ (2002) Behaviour of Fe-oxides relevant to contaminant uptake in the environment. *Chemical Geology* **190**, 321–337.
Taillefert M, Bono AB, Luther GW (2000) Reactivity of freshly formed Fe(III) in synthetic solutions and (pore) waters: Voltammetric evidence of an aging process. *Environmental Science and Technology* **34**, 2169–2177.
Tessier A, Fortin D, Belzile N, DeVitre RR, Leppard GG (1996) Metal sorption to diagenetic iron and manganese oxyhydroxides and associated organic matter: narrowing the gap between field and laboratory measurements. *Geochimica et Cosmochimica Acta* **60**, 387–404.
Torrent J, Schwertmann U, Barron V (1987) The reductive dissolution of synthetic goethite and hematite in dithionite. *Clay Minerals* **22**, 329–337.
Trolard F, Tardy Y (1987) The stabilities of gibbsite, boehmite, aluminous goethites and aluminous hematites in bauxites, ferricretes and laterites as a function of water activity, temperature and particle-size. *Geochimica et Cosmochimica Acta* **51**, 945–957.
Urrutia MM, Roden EE, Zachara JM (1999) Influence of aqueous and solid-phase Fe (II) complexants on microbial reduction of crystalline iron(III) oxides. *Environmental Science and Technology* **33**, 4022–4028.
Viollier E, Inglett PW, Hunter K, Roychoudhury AN, Van Cappellen P (2000) The ferrozine method revisited: Fe(II)/Fe(III) determination in natural waters. *Applied Geochemistry* **15**, 785–790.

Walker JCG, Klein C, Schidlowski M, Schopf JW, Stevensen DJ, Walter MR (1983) Environmental evolution of the Archean–Early Proterozoic Earth. In *Earth's Earliest Biosphere* (ed. Schoft JW). Princeton University Press, Princeton, New Jersey, pp. 260–290.

Welch SA, Barker WW, Banfield JF (1999) Microbial extracellular polysaccharides and plagioclase dissolution. *Geochimica et Cosmochimica Acta* **63**, 1405–1419.

Zachara JM, Fredrickson JK, Li SM, Kennedy DW, Smith SC, Gassman PL (1998) Bacterial reduction of crystalline Fe3+ oxides in single phase suspensions and subsurface materials. *American Mineralogist* **83**, 1426–1443.

Zachara JM, Fredrickson JK, Smith SC, Gassman PL (2001) Solubilization of Fe(III) oxide-bound trace metals by a dissimilatory Fe(III) reducing bacterium. *Geochimica et Cosmochimica Acta* **65**, 75–93.

Zachara JM, Kukkadapu RK, Fredrickson JK, Gorby YA, Smith SC (2002) Biomineralization of poorly crystalline Fe(III) oxides by dissimilatory metal reducing bacteria (DMRB). *Geomicrobiology Journal* **19**, 179–207.